Surface structure of Y_2O_3(9.5 mol %)-stabilized ZrO_2(001) determined by high-resolution medium-energy ion scattering

T. Nishimura, H. Toi, Y. Hoshino, E. Toyoda, and Y. Kido*
Department of Physics, Ritsumeikan University, Kusatsu, Shiga-ken 525-8577, Japan
(Received 29 January 2001; published 27 July 2001)

The surface structure of single crystalline ZrO_2(001) stabilized with Y_2O_3(9.5 mol %)(YSZ) was determined by high-resolution medium-energy ion scattering (MEIS). The clean 1×1 surface was prepared by a chemical treatment followed by annealing at 600 °C in O_2 atmosphere (1×10^{-5} Torr). The ion channeling combined with the blocking effect using 80-keV He^+ ions showed that the surface is strongly reconstructed and takes the form of a rumpled Zr(Y)O plane, where the O atoms are located on the center of the square of the Zr(Y) sublattice. The positions of the top layer O and Zr(Y) atoms measured from the underlying Zr(Y) plane are displaced toward the vacuum side by 0.11 ± 0.04 and 0.045 ± 0.02 Å, respectively, compared with the bulk interplanar distance. Analysis by the impact collision ion scattering spectroscopy using 1.8-keV He^+ ions supported the above surface structure and suggested that about 10% of the top layer O sites are vacant. The present MEIS analysis also revealed the fact that the thermal vibration amplitude of the top layer Zr(Y) atoms is strongly enhanced more than twice the bulk thermal vibration amplitude estimated from the simple Debye model. Such a low Debye temperature of the top surface is responsible for the strongly reconstructed surface structure with considerable O vacancies.

DOI: 10.1103/PhysRevB.64.073404 PACS number(s): 68.35.Dv, 61.85.+p, 68.35.Ja

Y_2O_3($7-20$ mol %)-stabilized ZrO_2 (YSZ) takes a cubic CaF_2-type structure with lattice constant of 5.14–5.17 Å.[1,2] Upon applications, YSZ is one of the most important superionic conductors for oxygen sensors and solid oxide fuel cells, due to its high oxygen-ion conductivity at elevating temperatures.[3,4] In addition, the fine-grained YSZ polycrystalline ceramics have a superplastic nature and the nanocrystallite powders are typically used as the starting material.[5] In spite of the vast technological relevance of YSZ, there have been very few studies of the surface properties.[2,6,7] In particular, the fundamental issue concerning the structure of the clean YSZ surface is entirely unknown.

In the present work, we prepared the clean 1×1 surface of YSZ(001) and determined the reconstructed surface structure by high-resolution medium-energy ion scattering (MEIS). The mirror-finished single-crystal Y_2O_3(9.5 mol %)-stabilized ZrO_2(001) with a size of $10\times10\times1$ mm^3 was purchased from Shinkosha Corporation. The elemental composition is $Zr_{1-x}Y_xO_{2-x/2}$ ($x=0.1735$) and 4.3% of the O sites is vacant in order to fulfill charge neutrality.[2,8] The surface was cleaned in a $H_2O_2(1)+H_2SO_4(1)$ for 5 min and then chemically etched with a solution of NH_4F(40%,139 g)+HF(47%,30 g) for 30 sec. The sample was immediately introduced into an ultrahigh vacuum chamber (2×10^{-10} Torr) and then annealed at 600 °C for 30 min in O_2 atmosphere (1×10^{-5} Torr). The Auger electron spectroscopy and low-energy ion scattering at glancing incidence showed no surface contaminations such as C. The reflective high-energy electron diffraction (RHEED) using a 30-keV electron beam gave a sharp 1×1 pattern accompanied by clear Kikuchi lines. It indicates a good quality of the surface crystallinity and the bulklike structure of the Zr(Y) sublattice. In the medium-energy ion scattering (MEIS) analysis, an 80-keV He^+ beam was used and the energies of backscattered ions were analyzed by a toroidal electrostatic analyzer (ESA) with an excellent energy resolution of $\Delta E/E=9\times10^{-4}$, which gives a monolayer depth resolution.[9,10] For more surface sensitive analysis, we employed the coaxial impact collision ion scattering spectroscopy (CAICISS) using a time-of-flight technique. The former determines precisely the positions of the reconstructed top layer atoms and the latter gives the information about the atomic species of the top layer and the approximate atomic configuration of near surface regions. In order to suppress the charge-up effect, the sample was heated to 150 °C during the RHEED and ion scattering experiments.

A preliminary analysis by CAICISS suggested that the top layer is comprised of O atoms, which were not located on the bulklike position. The detail of the CAICISS analysis will be described later. Considering a symmetric nature and vacant space, it is expected that the top layer O atoms take the position on the center of the square of the second layer Zr(Y) plane (see Fig. 1). In order to confirm such an atomic configuration, the blocking effect using medium-energy He ions is available. So, we fixed the incident direction parallel to the [101] axis and performed the angular scan in the (010) plane for the scattering direction. Figure 2 shows a typical MEIS spectrum for 80-keV He^+ ions incident along the [101] axis and backscattered to the $[30\bar{1}]$ direction. The surface peak includes the scattering components from the second and fourth Zr(Y) layers. The best fit was obtained by varying appropriately the normalized scattering yield from the fourth layer Zr(Y) and the relative stopping power (S/S_Z, S_Z: Ziegler's stopping power[11]) and normalized straggling [$(\Omega/\Omega_B)^2$, Ω_B: Bohr straggling] values. Judging from our data of surface peak analysis for $SrTiO_3$(001), RbI(001), and $NiSi_2/Si$(111),[12–14] the S/S_Z and $(\Omega/\Omega_B)^2$ values range from 1.2 to 2.0 and from 0.25 to 0.35. Such a large stopping power is ascribed to the fact that the detected ions passed through lattice atoms with small impact parameters in chan-

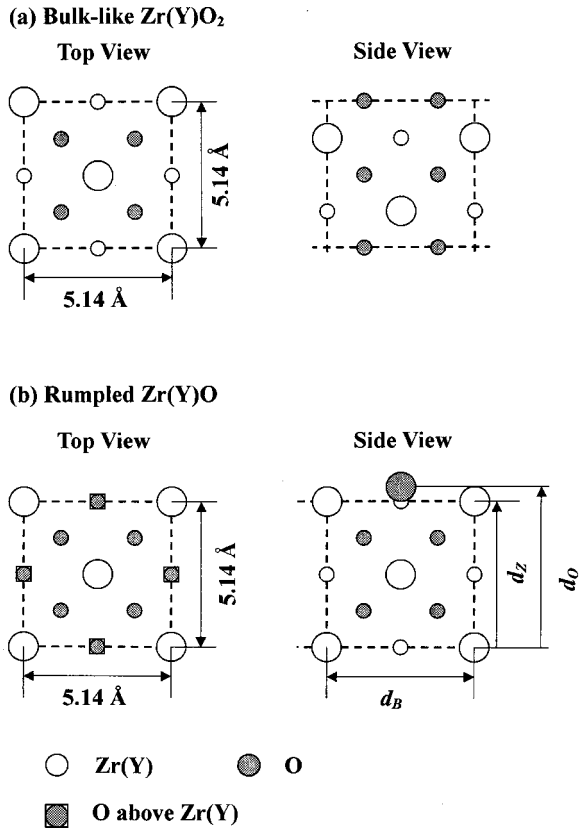

FIG. 1. Top and side views of YSZ(001) with (a) bulklike $Zr(Y)O_2$ and (b) rumpled Zr(Y)O face. Open and full circles denote O and Zr(Y) atoms, respectively and an open square overlapping a full circle indicates that a top layer O atom is located above a fourth layer Zr(Y) atom.

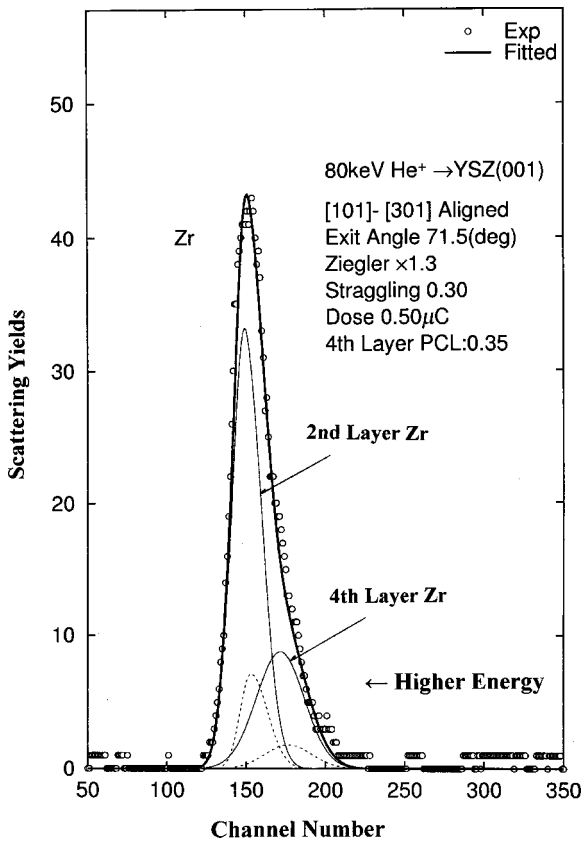

FIG. 2. Observed (open circles) and best-fitted (solid curve) MEIS spectra for 80-keV He^+ ions incident along the [101] axis and backscattered to the $[30\bar{1}]$ direction. Thin solid and dashed curves correspond to deconvoluted spectra from Zr and Y atoms, respectively. The best fit was obtained assuming that the stopping power was 1.3 times the Ziegler's one and the normalized straggling was 0.3.

neling and blocking geometries. Thus the scattering yield from the fourth layer Zr(Y) normalized by that from the second layer Zr(Y) was estimated to be 0.35. The normalized scattering yields from deeper layers ($\geqslant 6$) are negligibly small (less than 0.01). Such a large scattering component from the fourth layer Zr(Y), in spite of the double alignment condition, suggests strongly enhanced thermal vibration amplitudes and surface relaxation of the second layer Zr(Y) atoms. The angular scan spectra for the scattering yields from the second, fourth, and deeper layer Zr(Y) atoms are shown in Fig. 3(a). The angular dips seen at the exit angle of 71.4 (71.5)° for the scattering components from the fourth and deeper layers correspond just to the $[30\bar{1}]$ blocking direction (see Fig. 4). Other angular dips were also observed at $62.5\pm0.3°$ and $63.3\pm0.3°$ for the scattering components from the fourth and deeper Zr(Y) layers, respectively. The latter reflects the $[20\bar{1}]$ blocking effect for the He^+ ions backscattered from the Zr(Y) atoms in the depth more than the sixth Zr(Y) layer. The former indicates the blocking by the top layer O atoms for the He ions backscattered from the fourth layer Zr(Y) atoms. Here, a narrow energy window was set for the scattering component from the fourth layer Zr(Y) atoms, excluding the scattering components from the deeper layers. As expected, this angular dip indicates that the top layer O atoms are located on the center of the square of the second layer Zr(Y) plane at a height of 0.11 ± 0.04 Å from the second layer Zr(Y) plane. Such an atomic configuration corresponds to a so-called rumpled Zr(Y)O face.[12] No significant blocking dip was observed for the angular scan in the (110) plane for the scattering component from both the second and fourth layer Zr(Y) atoms. It indicates that the top layer O atoms do not form a bulklike O sublattice.

We determine the relaxation of the surface Zr(Y) atoms by the angular scan around the [101] axis in the (010) plane.[12] Figure 3(b) shows the angular scan spectra for 80-keV He^+ ions incident along the [101] axis and backscattered to around the $[10\bar{1}]$ direction in the (010) plane. Two blocking dips are seen around 44.5 and 45.0 ° for the scattering components from the fourth and deeper layers Zr(Y) atoms, respectively. From the angular shift of $0.5\pm0.3°$, the second layer Zr(Y) atoms are expanded toward the vacuum side by 0.045 ± 0.02 Å compared to the bulk interplanar distance of 2.57 Å (Zr-Zr or O-O planes; see Fig. 4). If one takes the fourth layer Zr(Y) plane as the basis, the surface relaxation and rumpling of the Zr(Y)O face are determined to be $+3.0\pm1.0\%$ and $+2.5\pm2.0\%$, respectively. Here, the plus sign in the relaxation means the displacement toward the vacuum side and the plus sign in the rumpling indicates

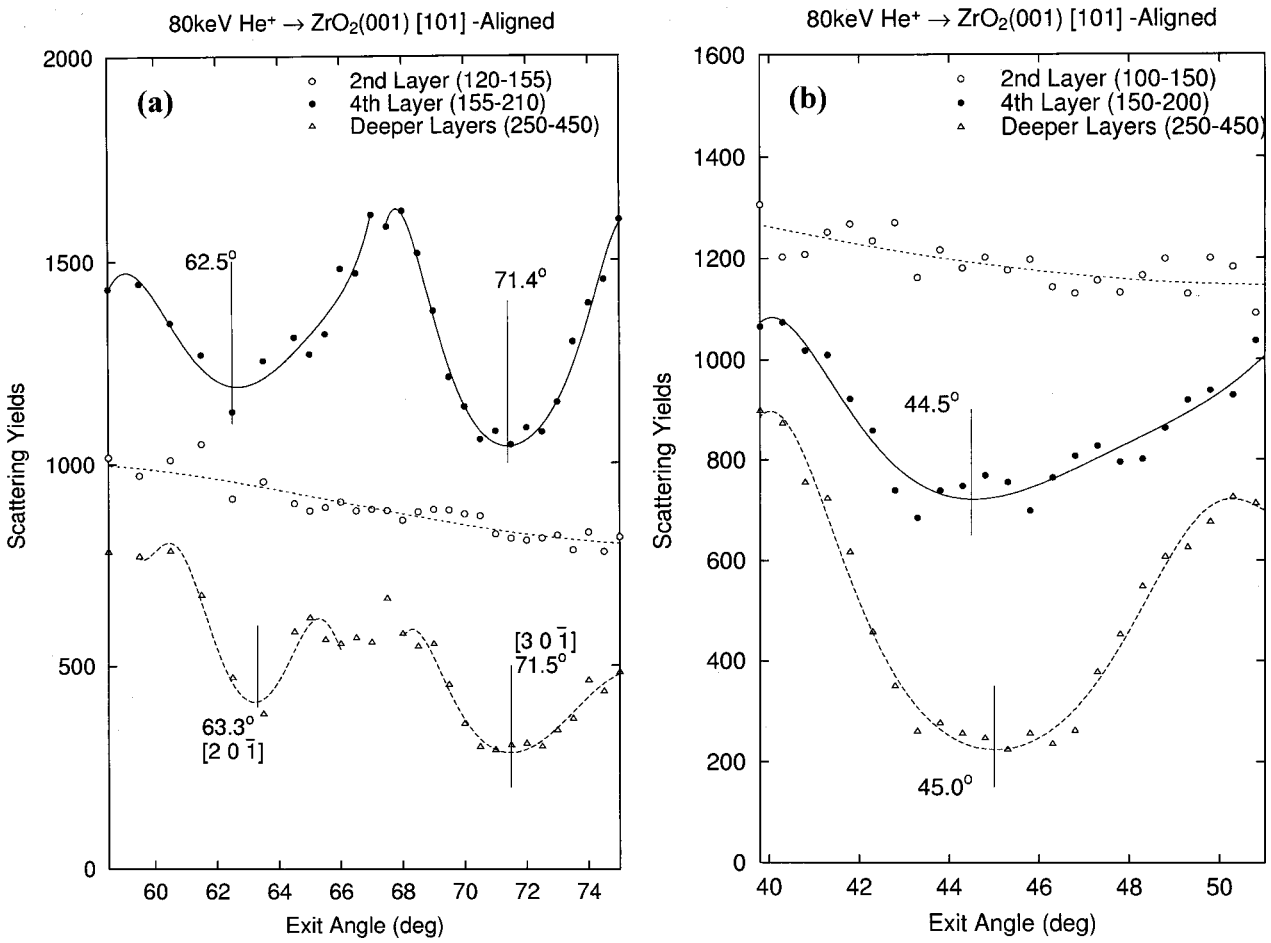

FIG. 3. Polar scan spectra for 80-keV He^+ ions incident along the [101] axis and backscattered to various directions in the (010) plane. Open and full circles and open triangles denote the scattering components from the second, fourth, and deeper layers Zr(Y), respectively. Each scattering component means the scattering yield divided by the differential scattering cross section. Solid, dotted, and dashed curves were obtained by polynomial fitting. (a) Polar scan around the $[20\bar{1}]$ and $[30\bar{1}]$ axes. (b) Polar scan around the $[10\bar{1}]$ axis.

the displacement of O atoms toward the vacuum side relative to that of Zr(Y) atoms.

We confirmed the rumpled Zr(Y)O face by CAICISS considering the ratios of the scattering yield from O to that from Zr(Y) atoms. Figure 5 shows the CAICISS spectrum for 1.8-keV He^+ ions incident along the [001] axis and backscattered to 180°. The large background is originated from the scattering components from the deeper layers Zr(Y). The background was fitted by an appropriate polynomial. Table I lists the ratios of the number of Zr(Y) atoms to that of O atoms seen for the [001], [101], and [111] incidence. Calculations were also performed assuming the bulklike $Zr(Y)O_2$ (O: top) and rumpled Zr(Y)O surface. In the case of the [101] incidence, the close encounter (hitting) probabilities[15] for the third layer O atoms are enhanced to 1.17 and 1.055, respectively, by the focusing effect owing to the second layer Zr(Y) and the top layer O atoms. The uncertainties are pronounced for the [101] and [111] incidence, because the O peak appears around the background maximum in the former case and the background intensity relative to the Zr(Y) surface peak intensity is large in the latter case. Apparently, overall agreement is obtained for the rumpled Zr(Y)O face. The assumption that about 10% of the top layer O sites are vacant leads to better agreement.

Recently, Herman[16] reported that $CeO_2(001)$ with a CaF_2-type lattice has the (1×1) bulk-equivalent surface, terminated with 0.5 monolayer O atoms. Such a bulklike surface terminated with O atoms cannot explain both the angular dip around 62.5° and the ratios of the number of Zr(Y) atoms to that of O atoms in the [001] CAICISS spectrum, as mentioned above. The reason why such difference occurs is

TABLE I. Ratios of number of O atoms to that of Zr(Y) atoms seen for the [001], [101], and [111] incidence. Calculations were performed assuming bulklike $Zr(Y)O_2$ (Zr and O, top) and rumpled Zr(Y)O surfaces. Values in parentheses are calculated ones assuming that 10% of the top layer O sites are vacant.

Incidence	O/Zr: observed	O/Zr: bulklike (Zr, top)	O/Zr: bulklike (O, top)	O/Zr: rumpled
[001]	2.4±0.3	2/2	2/2	3 (2.6)
[101]	3.7±0.4	2/1	2/1	3.5 (3.4)
[111]	1.8±0.4	1/1	2/0	1 (1)

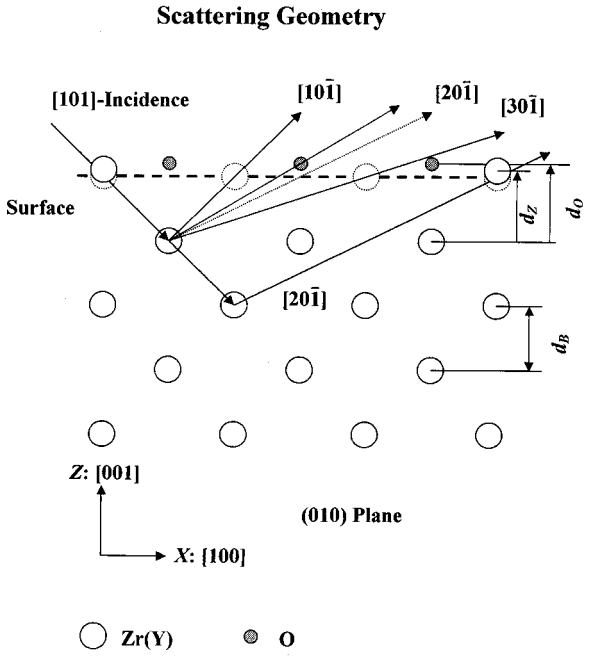

FIG. 4. Side view of the rumpled surface seen from the [010] axis. 80-keV He^+ ions are incident along the [101] axis and backscattered to various directions in the (010) plane.

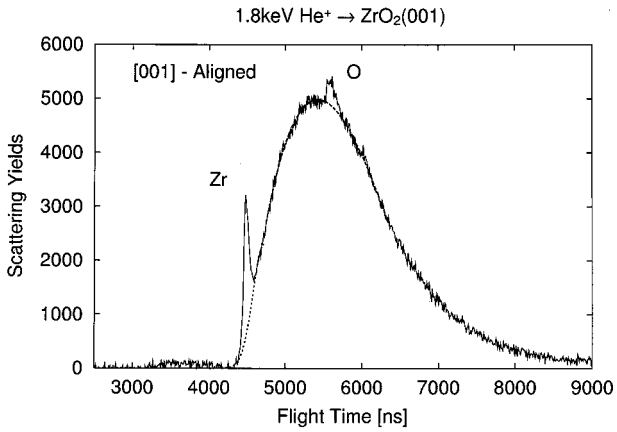

FIG. 5. CAICISS spectrum for 1.8-keV He^+ incident along the [001] axis and backscattered to 180°. The dashed curve denotes an appropriate polynomial fitted to the background originating primarily from backscattering from deeper layers Zr(Y) atoms.

not clear but we must note that in the heavily doped YSZ, the Zr atoms neighboring to an O vacancy are displaced from the ideal fluorite lattice and significant distortion is induced.[1,17]

In summary, the surface structure of Y_2O_3(9.5 mol %)-stabilized ZrO_2(001) was determined by high-resolution MEIS. The clean 1×1 surface was prepared by chemical etching in the buffered NH_4F-HF solution followed by annealing at 600 °C for 30 min in O_2 atmosphere (1×10^{-5} Torr). The surface takes the form of a rumpled Zr(Y)O plane, where the O atoms are located on the center of the square of the nonreconstructed Zr(Y) sublattice. The positions of the top layer O and Zr(Y) atoms are displaced toward the vacuum side by 0.11 ± 0.04 and 0.045 ± 0.02 Å, respectively, compared with the bulk interplanar distance. The CAICISS analysis using 1.8-keV He^+ ions supports the above surface structure and also suggests that about 10% of the top layer O sites are vacant. The present MEIS analysis has also revealed the fact that the thermal vibration amplitude of the top layer Zr(Y) atoms is strongly enhanced more than twice the bulk thermal vibration amplitude estimated from the simple Debye model. Such a low Debye temperature of the top surface is ascribed to the strongly reconstructed surface structure with considerable O vacancies.

The authors would like to thank Dr. M. Asari for useful comments in setting up the CAICISS system. Experimental assistance of their colleagues, T. Okazawa and Y. Taki, is greatly acknowledged.

*Corresponding author. Fax: +81-77-561-2657; email address: ykido@se.ritsumei.ac.jp

[1] Ping Li, I-Wei Chen, and J. E. Penner-Hahn, Phys. Rev. B **48**, 10 074 (1993).
[2] F. Parmigiani, L. E. Deperp, L. Sangaletti, and G. Samoggia, J. Electron Spectrosc. Relat. Phenom. **63**, 1 (1993).
[3] J. D. Solier, I. Cachadina, and A. D. Rodriguez, Phys. Rev. B **48**, 3704 (1993).
[4] S. J. Jiang, W. A. Schulze, V. R. W. Amarakoon, and G. C. Stangle, J. Mater. Res. **12**, 2374 (1997).
[5] T. Okubo and H. Nagamoto, J. Mater. Sci. **30**, 749 (1995).
[6] J. Nowotny, M. Sloma, and W. Weppner, Solid State Ionics **28–30**, 1445 (1988).
[7] W. C. Simpson, W. K. Wang, J. A. Yarmoff, and T. M. Orlando, Surf. Sci. **423**, 225 (1999).
[8] C. B. Azzoni, P. Camagni, and G. Samoggia, Sens. Mater. **8**, 209 (1996).
[9] T. Nishimura, A. Ikeda, and Y. Kido, Rev. Sci. Instrum. **69**, 1671 (1998).
[10] Y. Kido, T. Nishimura, Y. Hoshino, and H. Namba, Nucl. Instrum. Methods Phys. Res. B **161–163**, 371 (2000).
[11] J. F. Ziegler, J. P. Biersack, and W. Littmark, *The Stopping and Range of Ions in Matter* (Pergamon, New York, 1985).
[12] T. Nishimura, A. Ikeda, H. Namba, and Y. Kido, Surf. Sci. **411**, L834 (1998).
[13] A. Ikeda, T. Nishimura, T. Morishita, and Y. Kido, Surf. Sci. **433–435**, 520 (1999).
[14] Y. Kido, T. Nishimura, Y. Hoshino, E. Toyoda, and T. Nakada (unpublished).
[15] J. F. van der Veen, Surf. Sci. Rep. **5**, 199 (1985).
[16] G. S. Herman, Phys. Rev. B **59**, 14 899 (1999).
[17] D. Steele and B. E. F. Fender, J. Phys. C **7**, 1 (1974).